Biosorption of Cr(VI) by coconut coir: Spectroscopic investigation on the reaction mechanism of Cr(VI) with lignocellulosic material

Ying-Shuian Shen[a], Shan-Li Wang[a,*], Shiuh-Tsuen Huang[a,b], Yu-Min Tzou[a], Jang-Hung Huang[a]

[a] Department of Soil and Environmental Sciences, National Chung Hsing University, 250 Kuo Kuang Road, Taichung 40227, Taiwan
[b] Department of Science Application and Dissemination, National Taichung University, Taichung, Taiwan

ABSTRACT

In this study, the removal mechanism of Cr(VI) from water by coconut coir (CC) was investigated using X-ray photoelectron spectroscopy (XPS), Cr K-edge X-ray absorption near edge structure (XANES) and FTIR spectroscopy. The results showed that, upon reaction with CC at pH 3, Cr(VI) was reduced to Cr(III), which was either bound to CC or released back into solution. As revealed by the FTIR spectra of CC before and after reacting with Cr(VI), the phenolic methoxyl and hydroxyl groups of lignin in CC are the dominant drivers of Cr(VI) reduction, giving rise to carbonyl and carboxyl groups on CC. These functional groups can subsequently provide binding sites for Cr(III) resulting from Cr(VI) reduction. In conjunction with forming complexes with carbonyl and carboxyl groups, the formation of Cr(III) hydroxide precipitate could also readily occur as revealed by the linear combination fitting of the Cr K-edge XANES spectrum using a set of reference compounds. The phenolic groups in lignin are responsible for initiating Cr(VI) reduction, so lignocellulosic materials containing a higher amount of phenolic groups are expected to be more effective scavengers for removal of Cr(VI) from the environment.

© 2010 Elsevier B.V. All rights reserved.

1. Introduction

Pollution of surface and ground water supplies with toxic Cr(VI) has been one of the major causes for the deterioration in water quality. The origin of Cr(VI) in the environment is predominantly anthropogenic and the major source of Cr(VI) pollution is wastewater released from the industries that use Cr(VI), such as the electroplating, leather tanning and wood preservation industries [1,2]. Due to the high toxicity and carcinogenicity of Cr(VI) [3], protection of water resource from Cr(VI) pollution is an important task for healthy living. The current drinking water guideline value for Cr(VI) recommended by the World Health Organization is $50\,\mu g\,L^{-1}$ [3]. Compliance with this strict standard is expected to be very costly, and therefore, treatment efficiency is one of the major concerns for risk management when treating water containing Cr(VI).

Of the conventional techniques for removing Cr(VI) from water, adsorption methods are considered to be the most advantageous due to their removal effectiveness, low cost and ease of handling. In the literature, many studies have suggested that crop residues containing lignocellulosic biomass are effective scavengers for Cr(VI) in water and extensive reviews can be seen in Bailey et al. [4], Kur-

niawan et al. [5], Mohan and Pittman [6], and Sud et al. [7]. Selected crop residues such as sugarcane bagasse [8], corncob [8], nut shells [9,10], straw and bran from rice and wheat [11,12], and coconut coir [13] have been tested for their Cr(VI) removal efficiency. These studies mainly focused on the Cr(VI) removal capacities of the materials, finding that each material's capacity depended on reaction time, solution pH, temperature and material dosage [4–7].

The mechanism of Cr(VI) removal by lignocellulosic biomass was previously attributed in the literature to anionic adsorption (e.g. [9,10]). Some studies also have pointed out that the reduction of Cr(VI) to Cr(III) by lignocellulosic biomass in crop residues may also contribute to Cr(VI) removal from water [8,11,14]. Because the remediation of Cr(VI) contamination should be based on the fundamental understanding of the reaction mechanism, this work attempted to clarify the mechanism of Cr(VI) reaction with lignocellulosic material. The model material selected for investigation was coconut coir (CC), which is available in a large quantity as a waste product from coconut production and has a high lignocellulose content [15]. For coconut coir (CC), Gonzalez et al. [13] reported a maximal Cr(VI) removal capacity of $6.3\,mg\,g^{-1}$, which decreased as the pH was increased. With the results of potentiometric titration, it was also suggested that the sorption sites were mainly associated with the phenolic groups [13]. In Namasivayam and Sureshkumar [16], the modification of CC by a cationic surfactant enhanced the removal capacity of CC for Cr(VI) and minor reduction of Cr(VI) to Cr(III) was observed during the removal process.

* Corresponding author. Tel.: +886 422840373x3406; fax: +886 422862043.
E-mail address: slwang@nchu.edu.tw (S.-L. Wang).

After CC or other lignocellulosic materials have been used to treat Cr(VI) contaminated waters, contaminant-bearing materials may be disposed of or treated to recover the contaminant. To develop effective methods for recycling the contaminant from used materials and to prevent the secondary pollution from the used materials during post-treatment processing requires an understanding of the manner in which the contaminant is bound to the materials. Higher treatment efficiency of contaminant-bearing materials will also lower the overall cost for treatment of contaminated waters. Therefore, our specific goal in this research was determination of the structure and oxidation state of Cr bound to the surface of CC after Cr(VI) reaction using Cr K-edge X-ray absorption near edge structure (XANES). The XANES of an absorbing element arises from the transitions of excited electrons to unoccupied electronic levels. This technique can provide information regarding the oxidation state and bonding character of the element [17,18]. FTIR spectroscopy was applied to determine which surface functional groups reacted with Cr. FTIR spectroscopy is very sensitive to changes in the compositions of functional groups in biomass [19], so it can be applied to observe the spectral perturbations associated with the changes in functional groups resulting from Cr(VI) reduction and to provide information about the sites reacting with the resultant Cr(III). These results will provide essential information for applying lignocellulosic materials to develop cost-effective technologies for removal of Cr(VI) from water and recycling of Cr from used materials.

2. Materials and methods

2.1. Sample preparation

Coconut coir (CC) was oven-dried at 60 °C for one week, ground and passed through a 0.5-mm sieve. The collected powder was then washed with deionized water and dialyzed in a cellulose ester tube for 1 week. The solids in the dialysis tube were then freeze-dried and stored in plastic bottles prior to use. The elemental composition of the CC sample was 43% C, 47% O, 6% H and 1% N as determined using a Heraeus elemental analyzer. The BET surface area was obtained to be $1.4 \, m^2 \, g^{-1}$ using a Micrometrics ASAP 2000 surface area analyzer with nitrogen adsorption at 77 K.

2.2. Cr(VI) removal of CC

A Cr(VI) stock solution with a concentration of $1000 \, mg \, L^{-1}$ was prepared by dissolving 1.867 g of K_2CrO_4 in 500 mL 0.01 M KCl solution. All the working solutions were subsequently prepared from this stock solution. The removal kinetics of Cr(VI) were studied at 25 °C in a 500-mL water-jacketed reaction vessel. Five hundred millilitres of a $50 \, mg \, L^{-1}$ Cr(VI) solution in 0.01 M KCl was first placed in the reaction vessel and pre-adjusted to pH 3 and 25 °C, and then 1 g of CC was added into the Cr(VI) solution under vigorously stirring. During the experiment, the solution pH was kept constant by adding 0.01 M KOH and HCl solutions as needed. Ten millilitres of aliquots were withdrawn from the suspension at given time intervals and filtered through a 0.45-µm cellulose-acetate membrane filter to collect the filtrates and solids. This filter exhibited negligible Cr(VI) reaction in the pre-test. The total Cr and Cr(VI) concentrations in the filtrates were determined using ICP-AES and the s-diphenylcarbazide (DPC) method [20], respectively. The difference between the total Cr and Cr(VI) concentrations in solution was attributed to the Cr(III) concentration. The amount of Cr bound to CC was calculated from the difference between the initial and measured concentrations of total Cr. The residual solids on filter membranes were washed with deionized water, freeze-dried and stored in plastic bottles for further spectroscopic analyses.

2.3. XPS and FTIR spectroscopy

The CC samples were analyzed using XPS and FTIR spectroscopy before and after Cr(VI) reaction. XPS analysis was carried out using PHI 5000 VersaProbe/Scanning ESCA Microprobe (ULVAC-PHI, Inc) with a Mg $K\alpha$ X-ray source. Transmission FTIR spectra were acquired for samples randomly distributed in a KBr pellet, using a ThermoNicolet Nexus FTIR spectrometer equipped with a MCT detector and a KBr beamsplitter. Spectra were obtained in the range of $4400–400 \, cm^{-1}$ by co-addition of 64 individual scans with an optical resolution of $4 \, cm^{-1}$.

2.4. Cr K-edge XANES

The measurement of Cr K-edge XANES was performed at the Beamline X17C in the National Synchrotron Radiation Research Center at Hsinchu, Taiwan. The beamline optics include a vertically collimating pre-mirror, a fixed-exit double crystal Si(1 1 1) monochromator and a toroidal focusing mirror. At least two fluorescence spectra were collected for each sample using a Lytle detector. Spectral processing and analysis were conducted using Athena [21] following the procedure suggested by Kelly et al. [22]. Briefly, all spectra were calibrated to the absorption edge of metallic Cr at 5989 eV (i.e., E_0). The spectra for each sample were then averaged, followed by background removal and normalization.

Linear combination fitting (LCF) was used to determine the combinations of standard spectra giving the best fit to the sample spectra [22]. The standard compounds used in this work were Cr acetate hydroxide $((CH_3CO_2)_7Cr_3(OH)_2)$, Cr acetylacetonate $((C_5H_8O_2)_3Cr)$, $Cr(OH)_3$, Cr_2O_3 and CrO_3. Cr acetate hydroxide (CrAH) and Cr acetylacetonate (CrAA) were purchased from Sigma–Aldrich. Cr_2O_3 and CrO_3 were purchased from Merck KGaA. These chemicals were used without further purification. To synthesize $Cr(OH)_3$, 60 mL of 1.5 M NaOH solution was quickly added to 20 mL of 1.5 M $CrCl_3$ solution under vigorously stirring, and the pH of the solution was adjusted to 9.7 [23]. The suspension was filtered and the collected solid was freeze-dried. The Cr K-edge XANES of these reference compounds were collected using the same procedure for the samples and subsequently used to fit the sample spectra. The LCF was conducted using Athena [21], and no energy shifts were permitted in the LCF algorithm. The goodness of a fit was evaluated using the R factor, defined as $\sum(\text{data-fit})^2/\sum(\text{data})^2$ (see Athena Users' Manual for details), where the sums are over the data points in the fitting region (i.e., -30 to 40 eV relative to E_0).

3. Results and discussion

Fig. 1 shows Cr(VI) removal by CC as a function of time at pH 3 and 25 °C. Under this set of experimental conditions, complete removal of $50 \, mg \, L^{-1}$ Cr(VI) from the solution was achieved in 12 h. At this point in time, the removed Cr(VI) was converted to the Cr(III) in solution and Cr bound to CC, accounting for 20.7% and 79.3% of the total Cr, respectively (Fig. 1). Afterwards, the amount of Cr bound to CC (VI) gradually decreased, resulting in an increase of the Cr(III) concentration in the solution. Because Cr(III) was not originally present in the solution, its presence indicated the reduction of Cr(VI) to Cr(III). A continuous increase of the Cr(III) concentration revealed that Cr(III) was also present in Cr bound to CC. This was confirmed by the XPS analysis (Fig. 2). The Cr 2p spectra of the CC sample after reaction with Cr(VI) for 24 h showed two peaks at 576.6 and 586.2 eV, corresponding to Cr $2p_{3/2}$ and $2p_{1/2}$ orbitals, respectively [24]. The values of these two peaks were consistent with those of Cr(III) in Cr_2O_3 (Fig. 2), but different from those reported for Cr(VI) (i.e., 579–581 eV and 589–590 eV) [24–26]. Thus, this XPS result apparently showed that Cr bound to CC was pre-
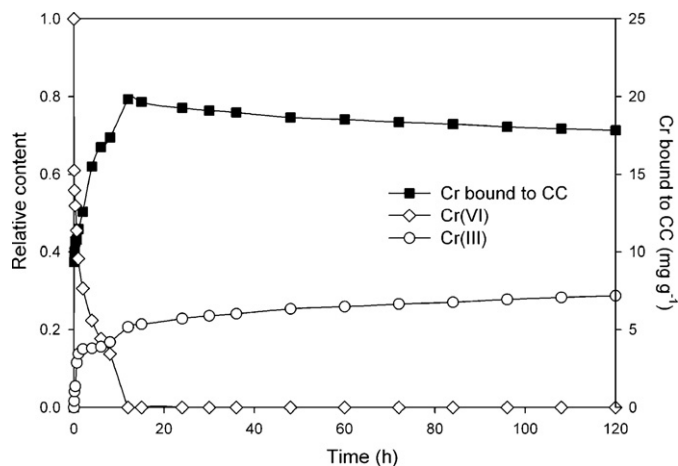
Fig. 1. Distribution of Cr(VI) and Cr(III) in solution and Cr bound to CC as a function of reaction time at pH 3 and 25 °C.

dominately in the trivalent form. Since the oxidation states of Cr in solution and Cr bound to CC were both in trivalent form, the reaction mechanism of Cr(VI) with CC was solely the reductive transformation of Cr(VI) to Cr(III) which was either released back to solution or sorbed on CC. The release of Cr(III) into the solution with the prolonged reaction time was probably due to the competition of aqueous K^+ and H^+ ions with sorbed Cr(III) ions for the surface binding sites on CC.

FTIR spectroscopy was applied to identify the functional groups of CC responsible for Cr(VI) reduction. To reveal the systematic changes in the spectral features upon Cr(VI) reaction, FTIR spectra were obtained for the sample after reacting with Cr(VI) for 0, 4, and 24 h (Fig. 3). The vibrations are contributed by the structures of cellulose, hemicellulose and lignin and their assignments are listed in Table 1 [27–29]. After CC reacted with Cr(VI), the intensities of the peaks at 1443, 1281, 863 and 819 cm^{-1} decreased while those at 1635 and 1556 cm^{-1} increased. The peaks at 1443 and 1281 cm^{-1} were attributed to the C–O–CH$_3$ (methoxyl) deformation and C–OH (hydroxyl) bending of phenolic structure in lignin and those at 863 and 819 cm^{-1} were assigned to the out-of-plane C–H bending vibrations of lignin (Table 1) [27–29]. Thus, the decreases in the intensities of these peaks indicated the oxidation of lignin in CC upon Cr(VI) reaction. In contrast, the intensities of the peaks contributed by cellulose and hemicellulose in CC were insignificantly affected by Cr(VI) reaction (Fig. 3 and Table 1). Therefore, lignin is taken to be the sole component in CC responsible for Cr(VI)
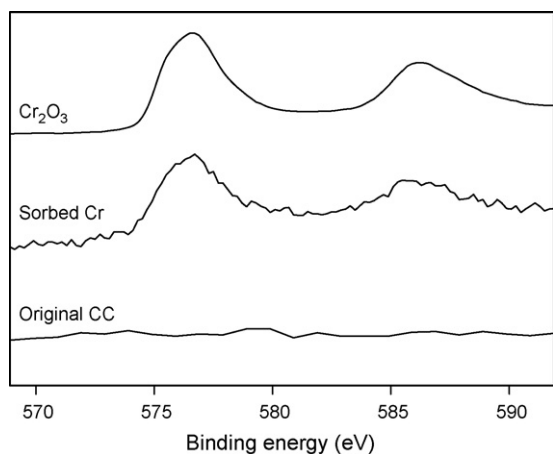

Fig. 2. Cr 2p X-ray photoelectron spectra of the original CC, Cr bound to CC after 24 h reaction time at pH 3 and Cr$_2$O$_3$.
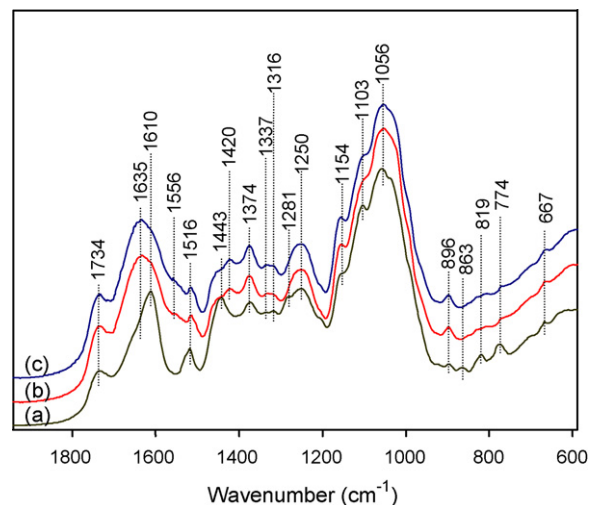

Fig. 3. FTIR spectra of the original CC (a) and CC after reacting with 50 mg L^{-1} Cr(VI) solution at pH 3 for 4 h (b) and 24 h (c).

reduction and the dominant functional groups in lignin driving the reaction are the phenolic methoxyl and hydroxyl groups. This conclusion is consistent with the mechanism of Cr(VI) reaction with coconut pith reported by Suksabye et al. [14]. Phenolic groups also play a key role in the Cr(VI) reduction of black carbon derived from lignocellulosic materials [30,31]. As suggested by Elovitz and Fish [32], the oxidation of phenols leads to the formation of quinones containing carbonyl groups. Further oxidation of quinones may lead to the formation of carboxylate anions [33]. Thus, upon Cr(VI) reaction, the increasing intensities at 1635 and 1556 cm^{-1} were attributed to the formation of carbonyl and carboxyl groups in CC (Fig. 3). The carboxyl and carbonyl groups may further provide the binding sites for Cr(III) resulting from Cr(VI) reduction.

The structure of Cr(III) bound to CC was determined using Cr *K*-edge XANES (Fig. 4a). The XANES spectra of CrAH, CrAA, Cr(OH)$_3$, Cr$_2$O$_3$ and CrO$_3$ were used as references for the known oxidation state and chemical species of Cr (Fig. 4b–f). CrO$_3$ was selected to serve as the reference standard for the Cr(VI) oxidation state (Fig. 4f), while the other compounds served as the references for the Cr(III) oxidation state in different coordination environments (Fig. 4b–e). In the XANES spectrum of CrO$_3$ (Fig. 4f), a single intensive pre-edge feature occurs at 5993.2 eV due to the transition of 1s electron to an unoccupied antibonding tetrahedral orbital [34,35]. This distinct character of Cr(VI) in tetrahe-

Table 1
IR absorption bands of coconut coir.

| Peak position (cm^{-1})	Assignment
1734	C=O stretching
1635	C=O stretching; HOH bending of water
1610	aromatic ring stretching
1516	C=C stretching
1443	C–O stretching; C–O–CH$_3$ deformation
1374	C–O and C–C stretching
1334	In-plane C–H deformation
1316	In-plane C–H deformation
1281	C–OH bending
1250	C–OH bending
1154	C–O–C stretching
1103	Ring skeletal C–O and C–C stretching
1056	Ring skeletal C–O and C–C stretching
896	C–H bending
863	Aromatic C–H out-of-plane bending
819	Aromatic C–H out-of-plane bending
774	Out-of-plane C–H and O–H bending
667	Out-of-plane C–H and O–H bending
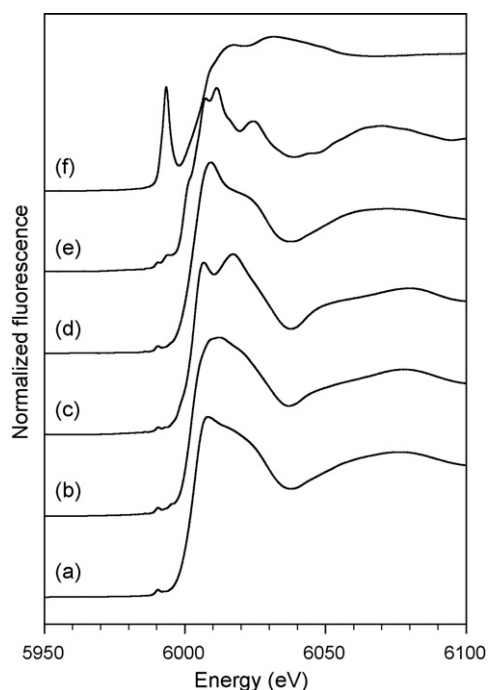
Fig. 4. Cr K-edge XANES for (a) CC collected after 24 h reaction time at pH 3, and the reference compounds (b) Cr acetate hydroxide, (c) Cr acetylacetonate, (d) $Cr(OH)_3$, (e) Cr_2O_3 and (f) CrO_3.

coordination can be used as an indicator of Cr(VI) in samples because, comparatively, only minor features are seen for Cr(III)-containing compounds (Fig. 4b–e). Accordingly, the absence of the strong pre-edge feature of Cr(VI) in the XANES spectrum for Cr bound to CC indicated that Cr(III) was the predominant oxidation state of Cr bound to CC. This finding was consistent with the result from XPS (Fig. 2).

The XANES spectra of the reference compounds containing Cr(III) show that even though Cr in these compounds is in the trivalent oxidation state, the corresponding spectral features in XANES are sensitive to changes in the bonding geometry of the Cr atom. The distinct features can therefore be applied to determine the bonding environment of Cr(III) bound to CC. By assuming that the reference compounds are representative of the actual species in the sample, the identification of each Cr(III) species can then be achieved by fitting the XANES spectra of the reference compounds. Because Cr(III) may be bound to carboxyl and carbonyl groups produced by the oxidation of phenolic groups as indicated by the results from FTIR spectroscopy, this complementary information was used to constrain the selection of standards to better

represent species in the sample; accordingly, CrAH (Fig. 4b) and CrAA (Fig. 4c) were selected as the reference compounds for Cr(III) binding to carboxyl and carbonyl groups, respectively. Meanwhile, in considering the possibility of forming surface precipitates on CC, the Cr K-edge XANES spectra were obtained for $Cr(OH)_3$ (Fig. 4d) and Cr_2O_3 (Fig. 4e) to serve as references for Cr(III) hydroxide and oxide precipitates, respectively. We then performed LCFs for the sample spectrum using the reference compounds. The results are listed in Table 2, following the order of the corresponding R factors.

As indicated by the R factor, the best fit was obtained when all four reference compounds were included in the model. In that case, the contributions of CrAH, CrAA, Cr_2O_3 and CrOH were 14.9%, 25.5%, 0% and 59.7%, respectively (model 1 in Table 2). The insignificant contribution of Cr_2O_3 indicated that it was possible to exclude this compound from the model. Accordingly, the result of the model 2, which included all the above reference compounds except Cr_2O_3, gave an R factor slightly larger than that of the model 1. As seen in Fig. 5A, the fit of model 2 was in good agreement with the sample spectrum. Similarly, comparison of the fitting results of models 3 and 5 with their counterparts without Cr_2O_3 (i.e., models 4 and 6, respectively) also showed no significant difference in their R factors. Meanwhile, among the models with only two reference compounds (models 4, 6 and 8–11), worse fits were obtained whenever Cr_2O_3 was included in the model (i.e., models 7, 8 and 11) (Table 2). Thus, Cr_2O_3 is unlikely to be the Cr(III) species bound to CC. In other words, $Cr(OH)_3$ is the only representative to Cr(III) precipitate on CC. Excluding $Cr(OH)_3$ from the model also resulted in more significant errors in the fits, as revealed by the greater values of the R factors in models 7–9 when compared with that of model 2 (Table 2). Thus, it is of certain that $Cr(OH)_3$ is present in the sample: a portion of the Cr(III) on CC forms $Cr(OH)_3$ precipitate and the remainder binds to CC through formation of complexes.

As indicated by the results from FTIR spectroscopy, the carboxyl and carbonyl groups in CC resulting from the oxidation of phenolic groups by Cr(VI) may provide the binding sites for Cr(III). To investigate whether carboxyl and carbonyl groups are both involved in the binding of Cr(III), either CrAH (model 4) or CrAA (model 6) was excluded from LCF and the results were compared with that of model 2, in which both CrAH and CrAA were used. A greater discrepancy between the experimental data and the fit was obtained for both models (Figs. 5B and C). Accordingly, the model 2 was considered to be the best fit to the sample spectrum (Fig. 5A). In this case, Cr precipitate and complexes compose of 59.6% and 40.4% of the Cr(III) species bound to CC, respectively (Table 2). Although the quantitative uncertainty of this result could be high, the qualitative result may be sound. That is, Cr(III) resulting from Cr(VI) reduction by CC may be bound to CC through forming hydroxide precipitate and complexing with carboxyl and carbonyl groups.

Table 2
LCF results for the XANES spectrum of Cr bound to CC at pH 3.

Model	No. of standard compounds	Proportion of the standards in the sample (%)						R factor ($\times 10^3$)[†]
		CrAH	CrAA	Sum of Cr complex	Cr_2O_3	$Cr(OH)_3$	Sum of Cr precipitates	
1	4	14.9 (2.7)	25.5 (1.5)	40.4	0 (3.6)	59.7 (1.8)	59.7	0.167
2	3	15.1 (2.7)	25.3 (3.2)	40.4		59.6 (1.8)	59.6	0.169
3	3		32.0 (1.0)	32.0	0 (1.5)	68.2 (1.0)	68.2	0.185
4	2		31.9 (1.0)	31.9		68.1 (1.0)	68.1	0.188
5	3	49.6 (2.4)		49.6	0 (3.4)	50.5 (2.4)	50.5	0.331
6	2	49.5 (2.4)		49.5		50.5 (2.4)	50.5	0.332
7	3	76.2 (3.9)	14.3 (3.1)	90.5	9.5 (5.0)		9.5	0.782
8	2	92.3 (1.7)		92.3	7.7 (1.7)		7.7	0.782
9	2	90.0 (3.2)	10.0 (3.2)	100				0.810
10	2			0	0	100.0	100.0	0.820
11	2		69.8 (2.0)	69.8	30.2 (2.0)		30.2	1.709

† The R factor is generated by the Athena software for evaluating the goodness of a fit. The lower the values the better fit.
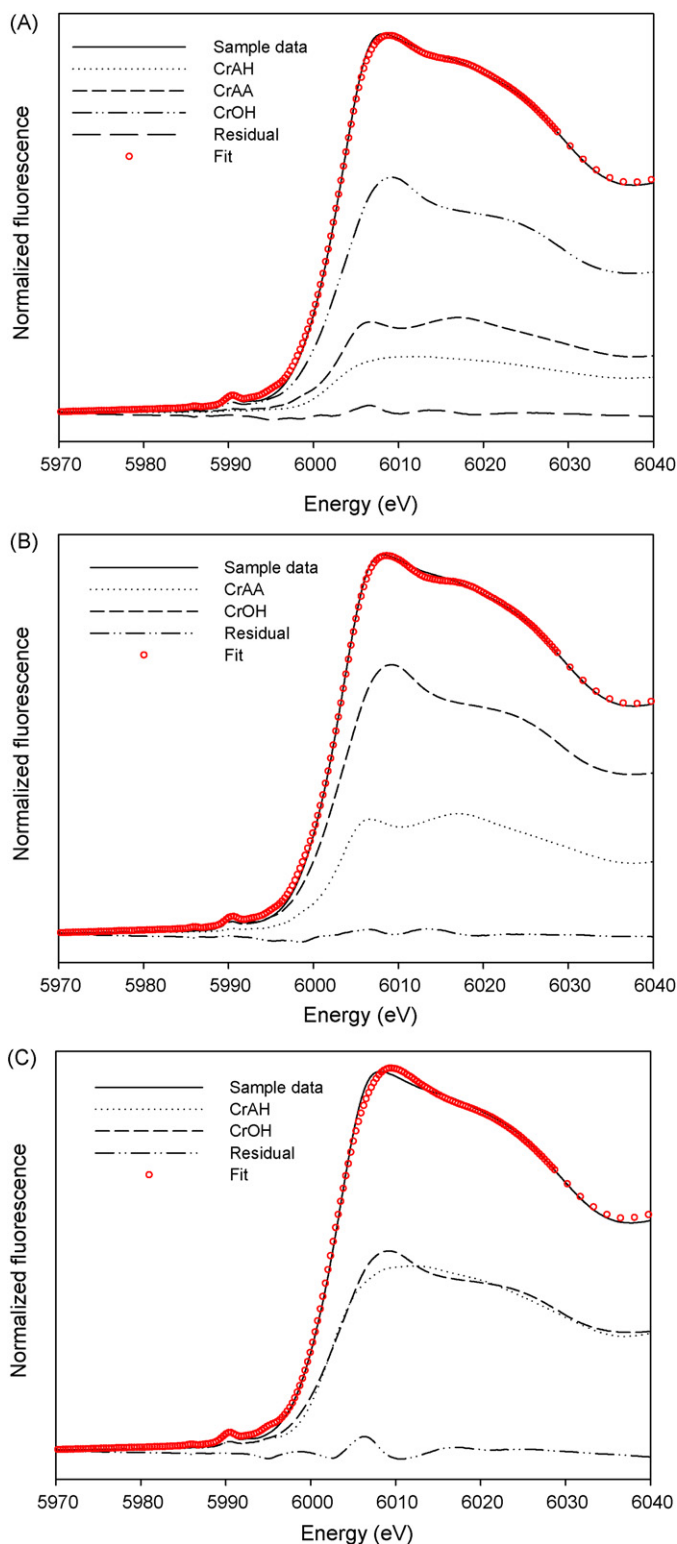
Fig. 5. XANES spectrum of CC collected after 24 h reaction time at pH 3, and the linear combination fits and component spectra of models 2, 4 and 6 in Table 2: (a) for model 2, the reference compounds CrAH, CrAA and Cr(OH)₃ were considered; (b) for model 4, CrAA and Cr(OH)₃ were considered; (c) for model 6, CrAH and Cr(OH)₃ were considered.

4. Conclusions

CC is an effective material in removing Cr(VI) from water. The mechanism of Cr(VI) removal is the reduction of Cr(VI) to Cr(III). The phenolic methoxyl and hydroxyl groups of lignin in CC are responsible for Cr(VI) reduction and the oxidation of these function groups gives rise to the formation of carbonyl and carboxyl groups on CC. These functional groups subsequently provide binding sites for Cr(III) ions resulting from Cr(VI) reduction. In addition to forming surface complexes, a portion of Cr(III) bound to CC also formed a hydroxide precipitate as revealed by the LCF of the corresponding Cr K-edge XANES spectrum using a set of reference compounds. Crop residues containing lignocellulosic biomass may provide wastewater industries with an abundant source of low-cost sorbents for the effective treatment and remediation of Cr(VI)-containing water because they can reduce toxic Cr(VI) to less toxic Cr(III). Since this ability of Cr(VI) reduction is contributed by the lignin component, a lignocellulosic material with a higher lignin content is expected to have a better performance in removing Cr(VI) from water.

References

[1] D.E. Kimbrough, Y. Cohen, A.M. Winer, L. Crelman, C. Mabuni, A critical assessment of chromium in the environment, Crit. Rev. Environ. Sci. Technol. 29 (1999) 1–46.
[2] J. Kotas, Z. Stasicka, Chromium occurrence in the environment and methods of its speciation, Environ. Pollut. 107 (2000) 263–283.
[3] WHO, Chromium in Drinking-water WHO/SDE/ESH/03.04/04, World Health Organization, Geneva, 2009.
[4] S.E. Bailey, T.J. Olin, R.M. Bricka, D.D. Adrian, A review of potentially low-cost sorbent for heavy metals, Water Res. 33 (1999) 2469–2479.
[5] T.A. Kurniawan, G.Y.S. Chan, W.H. Lo, S. Babel, Comparisons of low-cost adsorbents for treating wastewaters laden with heavy metals, Sci. Total Environ. 366 (2006) 409–426.
[6] D. Mohan, C.U. Pittman, Activated carbons and low cost adsorbents for remediation of tri- and hexavalent chromium from water, J. Hazard. Mater. B 137 (2006) 762–811.
[7] D. Sud, G. Mahajan, M.P. Kaur, Agricultural waste material as potential adsorbent for sequestering heavy metal ions from aqueous solutions—a review, Bioresour. Technol. 99 (2008) 6017–6027.
[8] U.K. Garg, M.P. Kaur, V.K. Garg, D. Sud, Removal of hexavalent chromium from aqueous solution by agricultural waste biomass, J. Hazard. Mater. 140 (2007) 60–68.
[9] M. Dakiky, M. Khamis, A. Manassra, M. Mer'eb, Selective adsorption of chromium(VI) in industrial wastewater using low-cost abundantly available adsorbents, Adv. Environ. Res. 6 (2002) 533–540.
[10] E. Pehlivan, T. Altun, Biosorption of chromium(VI) ion from aqueous solutions using walnut, hazelnut and almond shell, J. Hazard. Mater. 155 (2008) 378–384.
[11] L. Dupont, E. Guillon, Removal of hexavalent chromium with a lignocellulosic substrate extracted from wheat bran, Environ. Sci. Technol. 37 (2003) 4235–4241.
[12] H. Gao, Y. Liu, G. Zeng, W. Xu, T. Li, W. Xia, Characterization of Cr(VI) removal from aqueous solutions by a surplus agricultural waste–rice straw, J. Hazard. Mater. 150 (2008) 446–452.
[13] M.H. Gonzalez, G.C.L. Araujo, C.B. Pelizaro, E.A. Menezes, S.G. Lemos, G.B. de Sousa, A.R.A. Nogueira, Coconut coir as biosorbent for Cr(VI) removal from laboratory wastewater, J. Hazard. Mater. 159 (2008) 252–256.
[14] P. Suksabye, P. Thiravetyan, W. Nakbanpote, S. Chayabutra, Chromium removal from electroplating wastewater by coir pith, J. Hazard. Mater. 141 (2007) 637–644.
[15] C. Asasutjarit, S. Caroenvai, J. Hirunlabh, J. Khedari, Materials and mechanical properties of pretreated coir-based green composites, Composites B 40 (2009) 633–637.
[16] C. Namasivayam, M.V. Sureshkumar, Removal of chromium(VI) from water and wastewater using surfactant modified coconut coir pith as a biosorbent, Bioresour. Technol. 99 (2008) 2218–2225.
[17] P. Behrens, X-ray absorption spectroscopy in chemistry II. X-ray absorption near edge structure, Trend. Anal. Chem. 11 (1992) 237–244.
[18] J.G. Parsons, M.V. Aldrich, J.L. Gardea-Torresdey, Environmental and biological applications of extended X-ray absorption fine structure (EXAFS) and X-ray absorption near edge structure (XANES) spectroscopies, Appl. Spectrosc. Rev. 37 (2002) 187–222.

[19] C.T. Johnston, S.L. Wang, Application of vibrational spectroscopy in soil and environmental sciences, in: Handbook of Vibrational Spectroscopy, John Wiley and Sons, London, 2001, pp. 3192–3206.

[20] B.R. James, J.C. Petura, R.J. Vitale, G.R. Mussoline, Hexavalent chromium extraction from soils: a comparison of five methods, Environ. Sci. Technol. 29 (1995) 2377–2381.

[21] B. Ravel, M. Newville, ATHENA, ARTEMIS, HEPHAESTUS: data analysis for X-ray absorption spectroscopy using IFEFFIT, J. Synchrotron Radiat. 12 (2005) 537–541.

[22] S.D. Kelly, D. Hesterberg, B. Ravel, Analysis of soils and minerals using X-ray absorption spectroscopy, in: Methods of Soil Analysis Part 5. Mineralogical Methods, Soil Science Society of America, Madison, WI, USA, 2008, pp. 387–463.

[23] D. Rai, D.A. Moore, N.J. Hess, K.M. Rosso, L. Rao, S.M. Heald, Chromium(III) hydroxide solubility in the aqueous K^+–H^+–OH^-–CO_2–HCO_3^-–CO_3^{2-}–H_2O system: a thermodnyamic model, J. Solution Chem. 36 (2008) 1261–1285.

[24] E. Desimoni, C. Malitesta, P.G. Zambonin, J.C. Riviere, An X-ray photoelectron spectroscopic study of some chromium–oxygen systems, Surf. Interface Anal. 13 (1988) 173–179.

[25] A.R. Pratt, N.S. McIntyre, Comment on 'Curve fitting of Cr 2p photoelectron spectra of Cr_2O_3 and CrF_3', Surf. Interface Anal. 24 (1996) 529–530.

[26] I. Grohmann, E. Kemnitz, A. Lippitz, W.E.S. Unger, Curve fitting of Cr 2p photoelectron spectra of Cr_2O_3 and CrF_3, Surf. Interface Anal. 23 (1995) 887–891.

[27] R.K. Samal, B.B. Panda, S.K. Rout, M. Mohanty, Effect of chemical modification on FTIR spectra. I. Physical and chemical behavour of coir, J. Appl. Polym. Sci. 58 (1995) 745–752.

[28] K.K. Pandey, A study of chemical structures of soft and hardwood and wood polymers by FTIR spectroscopy, J. Appl. Polym. Sci. 71 (1999) 1969–1975.

[29] H. Yang, R. Yan, H. Chen, D.H. Lee, C. Zheng, Characteristics of hemicellulose, cellulose and lignin pyrolysis, Fuel 86 (2007) 1781–1788.

[30] N.H. Hsu, S.L. Wang, Y.C. Lin, G.D. Sheng, J.F. Lee, Reduction of Cr(VI) by crop-residue-derived black carbon, Environ. Sci. Technol. 43 (2009) 8801–8806.

[31] N.H. Hsu, S.L. Wang, Y.H. Liao, S.T. Huang, Y.M. Tzou, Y.M. Huang, Removal of hexavalent chromium from acidic aqueous solutions using rice straw-derived carbon, J. Hazard. Mater. 171 (2009) 1066–1070.

[32] M.S. Elovitz, W. Fish, Redox interactions of Cr(VI) and substituted phenols: products and mechanism, Environ. Sci. Technol. 29 (1995) 1933–1943.

[33] A. Santos, P. Yustos, A. Quintanilla, S. Rodriguez, F. Garcia-Ochoa, Route of the catalytic oxidation of phenol in aqueous phase, Appl. Catal. B 39 (2002) 97–113.

[34] A. Bianconi, E. Fritsch, G. Calas, J. Petiau, X-ray-absorption near-edge structure of 3d transition elements in tetrahedral coordination: the effect of bond-length variation, Phys. Rev. B 32 (1985) 4292–4295.

[35] I. Arcon, B. Mirtic, A. Kodre, Determination of valence states of chromium in calcium chromates by using X-ray absorption near-edge structure (XANES) spectroscopy, J. Am. Ceram. Soc. 81 (1998) 222–224.